ISSN 2377-1518

CANCER STUDIES AND MOLECULAR MEDICINE

Open Journal

Openventio PUBLISHERS

Original Research

Deep-Ultraviolet Raman Spectroscopy for Cancer Diagnostics: A Feasibility Study with Cell Lines and Tissues

Nicole M. Ralbovsky, BS[1]; Vladimir Egorov, PhD[2]; Eugene Moskovets, PhD[2]; Paromita Dey, MS[3]; Bijan K. Dey, PhD[3,4]; Igor K. Lednev, PhD[1,3,4*]

[1]*Department of Chemistry, University at Albany, SUNY, 1400 Washington Avenue, Albany, NY 12222, USA*
[2]*Advanced Tactile Imaging, Inc., 1457 Lower Ferry Rd, Trenton, NJ 08618, USA*
[3]*The RNA Institute, University at Albany, SUNY, 1400 Washington Avenue, Albany, NY 12222, USA*
[4]*Department of Biological Sciences, University at Albany, SUNY, 1400 Washington Avenue, Albany, NY 12222, USA*

[*]***Corresponding author***
Igor K. Lednev, PhD
Professor, Department of Chemistry, University at Albany, SUNY, 1400 Washington Avenue, Albany, NY 12222, USA; Tel. 518-591-8863; Fax. 518-442-3462; E-mail: ilednev@albany.edu

Article information
Received: March 22nd, 2019; **Revised:** April 8th, 2019; **Accepted:** April 15th, 2019; **Published:** April 15th, 2019

Cite this article
Ralbovsky NM, Egorov V, Moskovets E, Dey P, Dey BK, Lednev IK. Deep-ultraviolet Raman spectroscopy for cancer diagnostics: A feasibility study with cell lines and tissues. *Cancer Stud Mol Med Open J*. 2019; 5(1): 1-10. doi: 10.17140/CSMMOJ-5-126

ABSTRACT

Background
Deep-ultraviolet resonance Raman spectroscopy (UVRS) offers significant advantages over visible and near-infrared Raman spectroscopy for biological applications, including cancer identification. Cancer is the second-leading cause of death in the United States. Early diagnostics plays a crucial role in providing the best chances for an afflicted individual to seek successful treatment opportunities. Current methods for diagnosing various forms of cancer are both expensive and invasive. As such, the objective of this study is to explore the feasibility of UVRS for discrimination of cancerous tissues and cancer cells from normal samples. The safety issues of using ultraviolet light for human applications are analyzed.

Methods
Cancerous brain tissues from nonobese diabetic/severe combined immunodeficiency (NOD-SCID) model mice injected with 435-tdT cells (human adenocarcinoma breast cancer cells) at known locations and adjacent normal brain tissues as well as normal and cancer (adenocarcinoma PC-3) prostate cells were studied using UVRS. The obtained Raman spectra of the healthy and cancerous samples are compared in order to identify biochemical differences between them.

Results
The obtained spectra reflect biochemical differences which occur between the healthy and malignant samples in both brain and prostate cancers. UVRS provides distinctive resonance signatures of major biochemical components, including proteins and nucleic acids, and it does not suffer from fluorescence interference, nor does it require high laser power levels for excitation. These advantages allow for clear and effective spectral discrimination between samples.

Conclusion
Our results suggest UVRS should be considered for cancer identification, and is safe for use within humans. The proposed innovative approach has significant potential for cancer imaging and real-time tissue discrimination during surgery.

Keywords
Cancer diagnostics; Deep-ultraviolet resonance Raman spectroscopy; Prostate cancer; Brain cancer; Cancer imaging systems.

Abbreviations
UVRS: Deep-ultraviolet resonance Raman spectroscopy; RS: Raman spectroscopy; CARS: Coherent Anti-Stokes Raman Scattering; SRS: Stimulated Raman Scattering; UV: Ultraviolet; IR: Infrared.

Cancer Stud Mol Med Open J. 2019; 5(1): 1-10. doi: 10.17140/CSMMOJ-5-126

INTRODUCTION

Cancer is known as one of the most dreaded diagnoses a doctor can make. The time, pain, effort, and oftentimes heartache associated with a cancer diagnosis will undoubtedly impact most people, either directly or indirectly, at least once in their lifetime. Cancer is the second-leading cause of death in the United States, and in 2018 alone, 18.1 million new cases of cancer were identified.[1]

Current methods for diagnosing cancers generally include lab tests conducted on body fluids, imaging exams, and biopsies. These tests are time-consuming and invasive for the patient. Specific and accurate diagnoses are not always made, with the potential for misdiagnoses to occur. There remains a need for the development of a much more accurate and sensitive method which can universally diagnose cancer and could be used in cancer imaging systems during surgery.

Raman Spectroscopy (RS) is a powerful analytical technique that allows detection and measurement of basic molecular classes in complex biological samples, such as body fluids, cells, and tissues.[2-4] Therefore, the RS technique has a great potential for use as a diagnostic tool.[5,6] RS identifies chemical specificity of molecular species without staining or labeling. The RS spectral "signature" may be used to build multivariate calibration and classification models for practical clinical needs.[7,8] Raman signals from tissues originate from laser light backscattered by molecules. This allows for the collection of the backscattered light into the same optical fiber used for tissue illumination, which makes RS a practical tool for *in vivo* diagnostics and for examination of tissue specimens. RS system for tissue diagnostics can readily incorporate recent advances in the design of optical light collectors, miniaturization of lasers, and noise reduction in photon counting devices (e.g., cryogenically cooled charged coupled device (CCD) cameras). It is able to complement other techniques and, in many cases, provide new information unattainable by other approaches.[9-11] The ability of RS to recognize and quantify biological molecules (lipids, proteins, DNA, etc.) through their unique vibrational signatures has been well demonstrated.[12-19] Traditional RS has two main drawbacks: (1) a low efficiency (one RS photon is detected per 107 photons irradiating a sample) of the inelastic light scattering compared to elastic scattering[20,21] and (2) inherent fluorescence which accompanies RS studies.[22] For example, using a traditional 785 nm excitation for RS, one typically records low-level noisy Raman signals. Acquisition of a high-quality spectrum requires extended accumulation time with cryogenically cooled CCD cameras, which limits the application of RS for tissue imaging involving hundreds or thousands of spectral measurements.

Coherent anti-stokes Raman scattering (CARS) can improve the efficiency of RS.[23] In CARS, coherent vibrations of the molecules are driven at a selected frequency by simultaneous action of "pump" and "Stokes" lasers. The wavelength of a laser is fixed and that of another laser is tuned over a narrow range to excite the molecular vibrational mode of interest.[24-26] The major drawback of CARS is the existence of a non-resonant background.[27] Additionally, the CARS signal is decreased quadratically with the molecular concentration, making detection of low-abundance molecular species difficult. CARS requires the use of two rather expensive lasers generating picosecond pulses.[28] Also, due to a nonlinear physical process with ultra short laser pulses, a broadening of recorded Raman bands is observed, which can be detrimental to chemical specificity.[29] Because the signal generation in CARS critically depends on the tight overlap of the pump and Stokes laser foci, keeping this overlap constant can be problematic within the *in vivo* environment.[30]

Stimulated Raman Scattering (SRS) also utilizes "pump" and "Stokes" lasers to produce trains of picosecond pulses. When the difference between the frequencies of the "pump" and "Stokes" photons match the frequency of a molecular vibration, stimulated emission occurs; thus, the intensity of the pump laser transmitted by the specimen decreases while that of the Stokes beam increases. High-frequency modulation is used.[31,32] Though SRS showed a great promise in studying thin tissue slices and cell cultures,[33] its application to *in vivo* diagnostics has technical difficulties. The problem of keeping a tight overlap between the foci of two laser beams is also pertinent to SRS. Due to its nonlinear nature, the SRS signal is affected by variations in tissue composition (local density, presence of lipid droplets), non-Raman background, and photo damage.[34]

Deep-ultraviolet resonance Raman spectroscopy (UVRS) may be used as an alternative method for detecting cancer within biological specimens. It has been shown that a low RS yield can be dramatically increased by using excitation wavelengths near molecular electronic transitions (resonances).[35] The strength of Raman signals, caused by excitation of vibrational modes associated with that transition, exhibits an exponential increase.[36] The inelastic scattering by biological samples is increased many-fold around 200 nm due to strong electronic absorption of amide groups.[37] Accordingly, the use of ultraviolet (UV) excitation can cause a thousand-fold increase in the Raman signal because the Raman cross section increases by the 4th power of the excitation light frequency.[37] This makes UV resonance RS indispensable for studying protein structure and transformation,[38-40] understanding fibrils and fibrillogenesis,[41-44] analyzing bacteria and microorganisms,[45-47] and various other biological applications. Most importantly, the use of laser wavelengths below 250 nm eliminates the problem of autofluorescence which impedes Raman studies on tissues using near-infrared lasers.[48-50] Contrary to CARS and SRS, the UV resonance RS may simultaneously provide polychromatic information about Raman signatures of the tissue or body fluid being analyzed. An advanced processing of Raman spectra considerably improves tissue identification.[51] Overall, UV excitation allows significant reduction of irradiation power to address safety concerns and to generate high signal-to-noise ratios for Raman spectra, as well as decrease its accumulation time. These factors are of great importance for a new UVRS technology.

The objective of this study is to explore the feasibility for deep-ultraviolet resonance Raman spectroscopy to be used for cancer detection in prostate cancer cell lines and cancerous

brain tissues. Results show that UVRS is able to identify biochemical differences between malignant and healthy biological samples, thus opening the door for future studies to occur using UVRS for cancer imaging during surgery.

MATERIALS AND METHODS

Human Prostate Cell Culture

Normal human primary prostate epithelial cells (HPrEC) (ATCC® PCS-440-010™) and grade IV adenocarcinoma PC-3 prostate cancer cells (ATCC® CRL-1435™) were used for this study. The cells were obtained from the American Type Culture Collection (ATCC).

The HPrEC cells were cultured in 75 cm^2 tissue culture flask (Corning® T-75 flasks catalog #430641) using Complete Growth Medium (ATCC). To make the complete growth medium, L-Glutamine, Extract P, Epinephrine, rhTGF-a, Hydrocortisone hemisuccinate, rh Insulin and Apo-transferrin at a final concentration of 6 mM, 0.4%, 1.0 mM, 0.5 ng/mL, 100 ng/mL, 5 mg/mL, and 5 mg/mL respectively were added to the Prostate Epithelial Cell Basal Medium (ATCC® PCS-440-030™). The HPrEC cells were passaged when the cells reached approximately 80% confluency. The flask was rinsed twice with 5 mL D-PBS (ATCC 30-2200), and 5 mL pre-warmed trypsin-EDTA solution (ATCC® PCS-999-003) was added and incubated at 37 °C CO_2 incubator for 1-2 minutes. The flask was then gently tapped from all sides to facilitate detachment of the cells from the surface of the flask. An equal volume of the Trypsin Neutralizing Solution (ATCC PCS-999-004) was added to the flask and the cells were collected in a 15 mL tube. The tube containing the trypsin-EDTA-dissociated cells was centrifuged at 1000 rpm for 5 minutes. The solution was then aspirated from the cell pellet and the cells were resuspended in 10 mL of pre-warmed complete growth medium, at which point the cell numbers were counted. The cells were then seeded in a new tissue culture flask at a density of 5,000-6,000 viable cells per cm^2 and grown at 37 °C in a 5% CO_2 incubator for 2-3 days until they reached 80% confluency.

The PC-3 prostate cancer cells were cultured using Complete Growth Medium (ATCC). The base medium for this cell line is F-12K Medium (ATCC Catalog No. 30-2004). To make the complete growth medium, fetal bovine serum (ATCC) was added to this medium at a final concentration of 10%. The cells were cultured using 75 cm^2 tissue culture flask and subcultured following the similar procedures as described above for HPrEC cells.

Mouse Brain Tissues

The cancerous brain tissues were obtained from NOD-SCID-model mice injected with 435-tdT cells (human breast adenocarcinoma cancer cell line, MDA-MB-435)[52,53] were provided by Prof. V. Raman, Johns Hopkins University School of Medicine, (Baltimore, MD, USA).[54] The adjacent normal brain tissues were obtained for comparison. The characterization of such cancerous and normal brain tissue sections was carried out in an earlier study.[55]

Sample Preparation

The prostate cancer and healthy cell lines were received and analyzed immediately following cell culturing. For analysis, the cells were dispersed in about 150 μL of water.

The mice brain tissue was removed from the glass slide and separated into two tubes. One tube contained tissue from the identified normal tissue area and the other tube contained the cancerous tissue; the tissue cancer mapping was provided.[54] The tissue was mixed with 150 μL of water and sonicated to create a water dispersion.

Deep-UV Spectroscopic Methods

All samples were analyzed using a deep-UV Raman Spectrograph (details regarding instrument can be found elsewhere).[56] Briefly, 198-nm radiation was generated as the 5th anti-Stokes shift from the third harmonic of the Ni-YAG laser in a Raman shifter filled with low pressure hydrogen. A UV laser beam (~0.5 mW at the sample surface) was focused into a spinning Suprasil nuclear magnetic resonance (NMR) tube containing the solution. In order to prevent photo degradation, the solution was continuously mixed with a magnetic stirrer. Scattered radiation was collected in the backscattering geometry, dispersed using a double monochromator, and detected with a liquid-nitrogen cooled CCD camera (Roper Scientific, New Jersey, USA).

Data Acquisition and Treatment

For the collection of data from the cell samples, the accumulation time was 30 seconds, and 20 acquisitions were obtained and averaged for each spectrum. For the tissue samples, the accumulation time remained the same, however, 40 acquisitions were collected and averaged for each spectrum. The collection of multiple acquisitions per sample is conducted in order to account for the inherent heterogeneity of biological samples. The contribution of quartz from the NMR tube and of water was quantitatively subtracted from each spectrum. The spectra were preprocessed using GRAMS (version 9.2) software. Spectra were calibrated to wave numbers, using the Raman spectrum of Teflon as a reference, and smoothed.

RESULTS

Deep-UV resonance Raman spectra were collected from two different biological sample types. Tentative assignments were given to those bands observed in the Raman spectra using deep-UV excitation based on assignments from the literature which were obtained using near-IR and visible excitation.

First, prostate cancer and healthy cell lines were analyzed. The mean spectra for each of the two cell lines arepresent in Figure 1.

Figure 1. *Average Spectra Collected from Water Solutions of Normal Prostate Cells (Red) and Cancer Prostate Cells (Black) of a Human Using Deep-UV Raman Scattering*

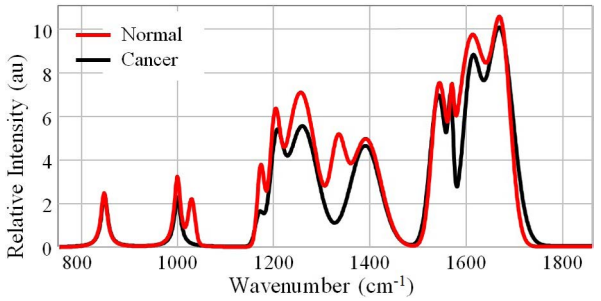

The spectra show general differences in protein structure and conformation, noted by variances in peak intensities at 1000, 1257, 1542, 1614, and 1669 cm^{-1}.[57,58] Collagen can tentatively be assigned as contributing to the Raman spectra at 1173, 1206, and 1334 cm^{-1}.[11,57,59] Various vibrational modes of DNA are observed at 1173, 1206, 1257, 1568, and 1614 cm^{-1} and by lipids at 1381 cm^{-1}.[60-62] Glycogen most likely contributes to the Raman spectrum as observed by the Raman bands at 850 and 1030 cm^{-1}.[57,63] A full list of tentative assignments for the vibrational modes of the various Raman bands is shown in Table 1.

Table 1. *Tentative Raman Shift Assignments of Spectra Collected From normal and Prostate Cancer Cell Lines Using UVRS*

Shift (cm^{-1})	Assignment	Contribution
850		Glycogen
1000	Phenylalanine symmetric ring breathing	Protein
1030		Glycogen
1173	Tyrosine, Cytosine; Guanine	Collagen; DNA
1206	Hydroxyproline, Tyrosine	Collagen; DNA
1257	Adenine and Thymine ring breathing; Amide III	DNA; Protein
1334	CH_3CH_2 Wagging	Collagen; Polynucleotide Chain
1381	CH_3 symmetric stretching	Lipids
1542	Amide II	Protein
1568	Guanine and Adenine ring breathing	DNA/RNA
1614	Tyrosine and Tryptophan C=C stretching; Adenine	Protein; DNA
1669	Amide I	Protein

Interestingly, the Raman bands have been assigned to vibrational modes of biomolecules which have previously been shown in the literature as playing a role in identifying prostate cancer. Many different protein biomarkers have been determined for detecting prostate cancer, including the prostate-specific antigen.[64,65] Collagen metabolism has been shown to be affected due to occurrence of prostate cancer, with the observed changes related to the grade of the tumor.[66-68]

The spectra of the two cell lines also reflect a decrease in glycogen and alterations in nucleic acid content, both of which have been previously reported by Crow et al as potential Raman spectroscopic markers for prostate cancer.[69,70] Various alterations in deoxyribonucleic acid (DNA) and ribonucleic acid (RNA) have been identified for signaling presence of the cancer, including in *PCA3* and the *TMPRSS2-ERG* gene fusion.[71]

The ability to detect variations in these classes of biomolecules indicates that UVRS is sensitive to the biochemical changes that occur during the pathogenesis of prostate cancer. These identified biomolecules serve as potential spectroscopic markers for cancer and should be further studied.

Next, sections of mouse brain tissues were analyzed. Figure 2 shows the spectra for cancerous and healthy tissues.

Figure 2. *Average Spectra Collected From Water Dispersions Of Healthy Brain Tissue (Red) And Cancer Brain Tissue (Black) Of A Mouse Using Deep-UV Raman Scattering*

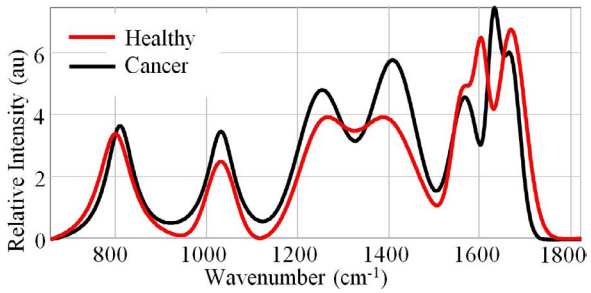

The spectra show great evidence of protein contribution, as designated by the Raman bands at 1260, 1400, 1602, 1630, and 1666 cm^{-1}.[57,72,73] Notably, the bands at 1630 and 1666 cm^{-1} differ greatly in intensity between the two average spectra. These bands correspond to the Amide I vibrational mode,[57] and the shift in wavelength indicates that the secondary structure of proteins in the tissue are generally undergoing a conformational change, suggesting proteins play a role in identifying brain cancer. In fact, many studies have already discovered proteins useful for identifying the presence or absence of brain cancer including thymosin β4, S100 calcium-binding protein A4, glial fibrillary acidic protein, epidermal growth factor receptor, peroxiredoxin 4, aldolase C fructose-biphosphate, and creatine kinase, to name a few.[74-76]

The influence of DNA and RNA to the Raman spectra of the two brain tissue areas are most likely denoted by peaks seen around 805 and 1570 cm^{-1}, and phospholipids contribute at 1032 cm^{-1}.[61,77-79] Nucleic acids and phospholipids have already been identified in previous Raman spectroscopic studies for contributing toward the identification of brain cancer within tissue samples.[80,81] Other studies have suggested certain RNA expression patterns as indicative of brain metastasis including ERCC1 and ERCC2 and long noncoding ribonucleic acid metastasis-associated lung adenocarcinoma transcript 1 (RNA MALAT1).[82,83] A full list of tentative Raman shift assignments for the brain tissue is presented in Table 2.

Table 2. *Tentative Raman Shift Assignments of Spectra Collected from Mouse Brain Tissue Using UVRS*

Shift (cm^{-1})	Assignment	Contribution
805	Uracil-based ring breathing; O-P-O stretching	RNA
1032	CH_2CH_3 bending	Phospholipids
1260	Amide III	Protein
1400	Aspartic and Glutamic acid (C=O) O^-stretching	Protein
1570	Guanine and Adenine ring breathing	DNA/RNA
1602	Phenylalanine and Tyrosine C=C in-plane bending	Protein
1630	Amide I	Protein
1666	Amide I	Protein

DISCUSSION

Raman spectroscopy, in general, has been widely studied for cancer identification purposes.[4,84,85] While a plethora of studies show the usefulness of near-IR and visible excitation of biological samples for detecting cancer, the advantages of UVRS spectroscopy have yet to be explored in terms of sensitivity, specificity and diagnostic accuracy. The UVRS approach is a promising and superior diagnostic method for cancer recognition due to the following factors. The excitation of biological samples in the wavelength range around 210-300 nm allows for the resonance enhancement of scattered light due to the amide chromophore, which is a crucial component of the backbone of a polypeptide; specifically, the polypeptide side chain including aromatic amino acids contributes to this enhancement.[86] The absorption spectra of aromatic amino acids typically exhibit peaks around 210-280 nm.[87] This overlap between absorption and excitation wavelengths result in the resonance enhancement of the Raman signal.[88,89] Aromatic amino acids have an inherent ability to probe the structure of the protein; with enhancement of these signals, the secondary structure of proteins is much more easily elucidated, allowing for this novel and specific information to aid in identifying malignancies. The resonance enhancement of nucleic acids has also been observed using deep-UV excitation. Mononucleotides exhibit resonance Raman enhancement at 266, 240, 218, and 200 nm UV radiation,[90,91] with various vibrational modes of the purine and pyrimidine bases observed in the resulting Raman spectrum. Again, the enhancement occurs due to the overlap between absorption and excitation wavelengths.[92] This information, which is not as well observed using near-IR or visible light excitation, provides a more specific insight into the biochemical changes that are occurring during the pathogenesis of cancers. Capitalizing on these advantages allows for a much greater potential to identify cancer within biological samples.

This proof-of-concept study contemplates the differences between single donors for two different types of cancer. While inherent inter-patient variability does exist, previous studies which have included multiple donors in each group have shown that the inter-patient variability is not significant enough to affect disease diagnostic efforts.[5,6] Furthermore, the Raman spectra for the four different biological samples shown here are dominated by protein and nucleic acid contributions. The inherent enhancement by deep-UV excitation provides crucial information regarding the differences which exist between healthy and cancerous biological samples. These differences can be translated to crucial biochemical information regarding cancer pathogenesis and may be useful for identifying cancer within patients in future studies.

Safety Considerations

There are great advantages for using UV excitation lasers, including eliminating broadband tissue autofluorescence, which arises after 255 nm (Figure 3) due to aromatic amino acids,[94,95,48] and increasing RS signals from proteins[97] and from lipids and fatty acids.[97,98]

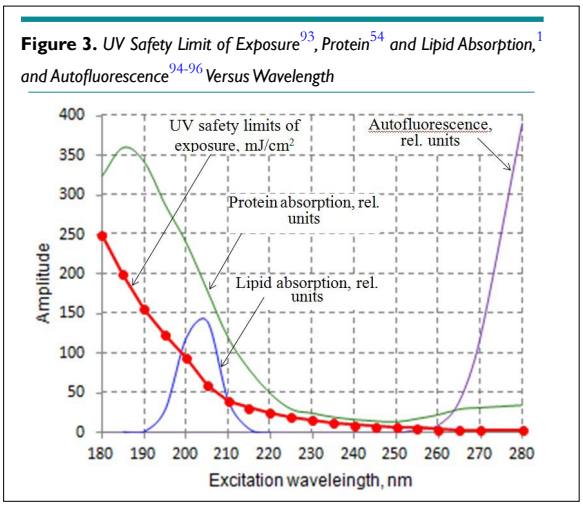

Figure 3. *UV Safety Limit of Exposure[93], Protein[54] and Lipid Absorption,[1] and Autofluorescence[94-96] Versus Wavelength*

However, shifting laser excitation to the deep-UV range brings about health risk issues, including photochemical damage of DNA.[99] The guidelines on safe UV exposure of human tissue/skin established by the International Commission on Non-Ionizing Radiation Protection (ICNIRP) indicate that exposure doses must be limited to 10 mJ/cm^2 for 240 nm and can be as high as 250 mJ/cm^2 for 180 nm (see red line, Figure 3).[93,100,101]

In this study, the UV radiation of a 0.4 mW laser was delivered and focused into a 7-μm spot (area ~50 μ^2) in the middle of a quartz tube filled with a water dispersion of either tissue or cells; the relative volume concentration of the cells was 0.5% (1:200). The UV Raman signal in our experiment was collected for 30 seconds using an optical system with 8% collection efficiency, and recorded by a UV CCD camera with an estimated detection efficiency of 5%.[60] Taking into account the small (0.5%) volume concentration of the cells in our experiment, we can derive, in the case where cells cover the entire sample area of 50 μ^2, the same level of Raman signal will be achieved after 30 s/200=0.15 s collection time. Accordingly, the energy density (i.e., energy per cm^2) of UV radiation for this area is 4×10^{-4} W$\times1.5\times10^{-1}$ s/(50×10^{-8} cm^2)=120 J/cm^2.

In future studies, the goal is to translate this work into the development of an efficient fiber-optic probe for UVRS-based cancer diagnostics of living tissues, which could map a living tissue in real time. As such, it is necessary to ensure that excitation by a deep-UV laser will not cause physiological problems. Assuming

that the sample area illuminated by the Raman probe is 300×300 μm^2 (~2000-fold larger than illuminated area in this study) and that photon collection efficiency of the Raman probe is approximately 20% we can calculate that, using the same UV laser, the radiation dose in the proposed approach is only 1:5000 of that in this study. This is equivalent to 120 $J/cm^2/5000=25$ mJ/cm^2, which is considered safe according to the ICNIRP guidelines discussed above.

To the best of our knowledge, this feasibility study demonstrates for the first time the ability of deep-UV Raman spectroscopy to discriminate cancerous from normal tissues and cells in a relatively short time with high sensitivity. The dramatic increase in sensitivity observed in our experiments, which cannot be obtained using near-IR or visible excitation, allows for identification of altered chemical/structure composition of cancerous versus normal conditions. This result may lead to a better understanding of changes which occur in a biochemical environment during the pathogenesis of cancer. The clear advantages of this method suggest that UVRS should be considered in future studies as a novel methodology for the specific and informative identification of cancer. Because it also meets safety guidelines for UV exposure, this method has the potential to be further developed into a real-time diagnostic method using fiber-optics.

CONCLUSION

This proof-of-concept study suggests deep-ultraviolet resonance Raman spectroscopy has significant potential for identifying cancerous and healthy biological species at both the cellular and tissue level. Many key advantages exist for using deep-UV excitation as compared to visible or near-IR excitation. Notably, deep-UV excitation provides resonance enhancement of crucial biochemical components and eliminates interference from fluorescence. These advantages allow for simple spectral interpretation, saving time and effort for the researcher which can be critical in diagnostic situations. Notably, changes in biochemical composition between healthy and prostate and brain cancer samples were discovered using UVRS. These differences can be capitalized on in future studies with larger sample sizes in order to further develop the method for identifying prostate and brain cancers. The proposed approach is shown to be a safe and effective method for detecting cancer within biological samples and provides a solid basis for research into further developing UVRS for clinical applications.

CONFLICT OF INTEREST

The authors declare that they have no conflicts of interest

REFERENCES

1. Bray F, Ferlay J, Soerjomataram I, Siegel RL, Torre LA, Jemal A. Global cancer statistics 2018: GLOBOCAN estimates of incidence and mortality worldwide for 36 cancers in 185 countries. *CA Cancer J Clin*. 2018; 68(6): 394-424. doi: 10.3322/caac.21492

2. Butler HJ, Ashton L, Bird B, et al. Using Raman spectroscopy to characterize biological materials. *Nat Protoc*. 2016; 11(4): 664-687. doi: 10.1038/nprot.2016.036

3. Harrison JP, Berry D. Vibrational spectroscopy for imaging single microbial cells in complex biological samples. *Front Microbiol*. 2017; 8: 675. doi: 10.3389/fmicb.2017.00675

4. Kong K, Kendall C, Stone N, Notingher I. Raman spectroscopy for medical diagnostics—From in-vitro biofluid assays to in-vivo cancer detection. *Adv Drug Deliv Rev*. 2015; 89: 121-134. doi: 10.1016/j.addr.2015.03.009

5. Ralbovsky N, Lednev IK. Raman hyperspectroscopy shows promise for diagnosis of Alzheimer's. *Biophotonics International*. 2018; 25(4): 33-37.

6. Ryzhikova E, Kazakov O, Halamkova L, et al. Raman spectroscopy of blood serum for Alzheimer's disease diagnostics: Specificity relative to other types of dementia. *J Biophotonics*. 2015; 8(7): 584-596. doi: 10.1002/jbio.201400060

7. Meksiarun P, Ishigaki M, Huck-Pezzei VAC, et al. Comparison of multivariate analysis methods for extracting the paraffin component from the paraffin-embedded cancer tissue spectra for Raman imaging. *Scientific Reports*. 2017; 7: 44890. doi: 10.1038/srep44890

8. Cals FL, Koljenović S, Hardillo JA, Baatenburg de Jong RJ, Bakker Schut TC, Puppels GJ. Development and validation of Raman spectroscopic classification models to discriminate tongue squamous cell carcinoma from non-tumorous tissue. *Oral Oncol*. 2016; 60: 41-47. doi: 10.1016/j.oraloncology.2016.06.012

9. Krafft C, Dietzek B, Popp J. Raman and CARS microspectroscopy of cells and tissues. *Analyst*. 2009; 134(6): 1046-1057. doi: 10.1039/b822354h

10. Kendall C, Isabelle M, Bazant-Hegemark F, et al. Vibrational spectroscopy: A clinical tool for cancer diagnostics. *Analyst*. 2009; 134(6): 1029-1045. doi: 10.1039/b822130h

11. Krafft C, Knetschke T, Siegner A, Funk RH, Salzer R. Mapping of single cells by near infrared Raman microspectroscopy. *Vibrational Spectroscopy*. 2003; 32(1): 75-83. doi: 10.1016/S0924-2031(03)00049-3

12. Rau JV, Graziani V, Fosca M, et al. RAMAN spectroscopy imaging improves the diagnosis of papillary thyroid carcinoma. *Scientific Reports*. 2016; 6: 35117. doi: 10.1038/srep35117

13. Lloyd GR, Orr LE, Christie-Brown J, et al. Discrimination between benign, primary and secondary malignancies in lymph nodes from the head and neck utilising Raman spectroscopy and multivariate analysis. *Analyst*. 2013; 138(14): 3900-3908. doi: 10.1039/c2an36579k

14. Shaikh R, Prabitha VG, Dora TK, et al. A comparative evaluation of diffuse reflectance and Raman spectroscopy in the detec-

tion of cervical cancer. *Journal of Biophotonics*. 2017; 10(2): 242-252.doi: 10.1002/jbio.201500248

15. Bakker Schut TC, Caspers PJ, Puppels GJ, et al. Discriminating basal cell carcinoma from its surrounding tissue by Raman spectroscopy. *J Invest Dermatol*. 2002; 119(1): 64-69. doi: 10.1046/j.1523-1747.2002.01807.x

16. Petersen D, Mavarani L, Niedieker D, et al. Virtual staining of colon cancer tissue by label-free Raman micro-spectroscopy. *Analyst*. 2017; 142(8): 1207-1215. doi: 10.1039/c6an02072k

17. Han B, Du Y, Fu T, et al. Differences and relationships between normal and atypical ductal hyperplasia, ductal carcinoma in situ, and invasive ductal carcinoma tissues in the breast based on Raman spectroscopy. *Appl Spectrosc*. 2017; 71(2): 300-307. doi: 10.1177/0003702816681009

18. Surmacki J, Musial J, Kordek R, Abramczyk H. Raman imaging at biological interfaces: Applications in breast cancer diagnosis. *Mol Cancer*. 2013; 12(1): 48. doi: 10.1186/1476-4598-12-48

19. Surmacki J, Brozek-Pluska B, Kordek R, Abramczyk H. The lipid-reactive oxygen species phenotype of breast cancer. Raman spectroscopy and mapping, PCA and PLSDA for invasive ductal carcinoma and invasive lobular carcinoma. Molecular tumorigenic mechanisms beyond Warburg effect. *Analyst*. 2015; 140(7): 2121-2133. doi: 10.1039/c4an01876a

20. López-Peña I, Leigh BS, Schlamadinger DE, Kim JE. Insights into protein structure and dynamics by ultraviolet and visible resonance Raman spectroscopy. *Biochemistry*. 2015; 54(31): 4770-4783. doi: 10.1021/acs.biochem.5b00514

21. Smith E, Dent G. Chapter 4: Resonance Raman Scattering. In: *Modern Raman Spectroscopy: A Practical Approach*. Hoboken, New Jersey, United States: John Wiley & Sons; 2005. 93-112.

22. Colaianni SM, Aubard J, Hansen SH, Nielsen OF. Raman spectroscopic studies of some biochemically relevant molecules. *Vibrational Spectroscopy*. 1995; 9(1): 111-120. doi: 10.1016/0924-2031(94)00066-P

23. Bocklitz TW, Salah FS, Vogler N, et al. Pseudo-HE images derived from CARS/TPEF/SHG multimodal imaging in combination with Raman-spectroscopy as a pathological screening tool. *BMC Cancer*. 2016; 16(1): 534. doi: 10.1186/s12885-016-2520-x

24. Evans CL, Potma EO, Puoris' haag M, Côté D, Lin CP, Xie XS. Chemical imaging of tissue *in vivo* with video-rate coherent anti-Stokes Raman scattering microscopy. *Proc Natl Acad Sci U S A*. 2005; 102(46): 16807-16812. doi: 10.1073/pnas.0508282102

25. Camp Jr CH, Jong Lee Y, Heddleston JM, et al. High-speed coherent Raman fingerprint imaging of biological tissues. *Nat Photonics*. 2014; 8(8): 627-634. doi: 10.1038/nphoton.2014.145

26. Kumar S, Kamali T, Levitte JM, et al. Single-pulse CARS based multimodal nonlinear optical microscope for bioimaging. *Opt Express*. 2015; 23(10): 13082-13098. doi: 10.1364/OE.23.013082

27. Popov K, Pegoraro A, Stolow A, Ramunno L. Image formation in CARS and SRS: Effect of an inhomogeneous nonresonant background medium. *Opt Lett*. 2012; 37(4): 473-475. doi: 10.1364/OL.37.000473

28. Potma EO, Xie XS. CARS microscopy for biology and medicine. *Optics and Photonics News*. 2004; 15(11): 40-45. doi: 10.1364/OPN.15.11.000040

29. Vartiainen EM, Rinia HA, Müller M, Bonn M. Direct extraction of Raman line-shapes from congested CARS spectra. *Opt Express*. 2006; 14(8): 3622-3630. doi: 10.1364/OE.14.003622

30. McVey A, Crain J. Nonlinear optical methods for cellular imaging and localization. *Methods*. 2014; 68(2): 371-377. doi: 10.1016/j.ymeth.2014.03.002

31. Freudiger CW, Min W, Saar BG, et al. Label-free biomedical imaging with high sensitivity by stimulated Raman scattering microscopy. *Science*. 2008; 322(5909): 1857-1861. doi: 10.1126/science.1165758

32. Francis A, Berry K, Chen Y, Figueroa B, Fu D. Label-free pathology by spectrally sliced femtosecond stimulated Raman scattering (SRS) microscopy. *PLoS One*. 2017; 12(5): e0178750. doi: 10.1371/journal.pone.0178750

33. Shen Y, Xu F, Wei L, Hu F, Min W. Live-cell quantitative imaging of proteome degradation by stimulated raman scattering. *Angew Chem Int Ed Engl*. 2014; 53(22): 5596-5599. doi: 10.1002/anie.201310725

34. Zhang D, Wang P, Slipchenko MN, Cheng J-X. Fast vibrational imaging of single cells and tissues by stimulated Raman scattering microscopy. *Acc Chem Res*. 2014; 47(8): 2282-2290. doi: 10.1021/ar400331q

35. Long DA. *The Raman Effect: A Unified Treatment of the Theory of Raman Scattering by Molecules*. Hoboken, New Jersey, USA: John Wiley & Sons, Ltd.; 2002.

36. Asher SA. UV resonance Raman studies of molecular structure and dynamics: Applications in physical and biophysical chemistry. *Annu Rev Phys Chem*. 1988; 39(1): 537-588. doi: 10.1146/annurev.pc.39.100188.002541

37. Carey PR. *Molecular Biology: Biochemical Applications of Raman and Resonance Raman Spectroscopies*. New York, USA: Academic Press. 1982.

38. Huang C-Y, Balakrishnan G, Spiro TG. Protein secondary structure from deep-UV resonance Raman spectroscopy. *Journal of Raman Spectroscopy*. 2006; 37(1-3): 277-282. doi: 10.1002/

jrs.1440

39. Shashilov VA, Sikirzhytski V, Popova LA, Lednev IK. Quantitative methods for structural characterization of proteins based on deep UV resonance Raman spectroscopy. *Methods*. 2010; 52(1): 23-37. doi: 10.1016/j.ymeth.2010.05.004

40. Xu M, Ermolenkov VV, He W, Uversky VN, Fredriksen L, Lednev IK. Lysozyme fibrillation: Deep UV Raman spectroscopic characterization of protein structural transformation. *Biopolymers*. 2005; 79(1): 58-61. doi: 10.1002/bip.20330

41. Popova LA, Kodali R, Wetzel R, Lednev IK. Structural variations in the cross-β core of amyloid β fibrils revealed by deep UV resonance Raman spectroscopy. *J Am Chem Soc*. 2010; 132(18): 6324-6328. doi: 10.1021/ja909074j

42. Shashilov VA, Lednev IK. 2D correlation deep UV resonance raman spectroscopy of early events of lysozyme fibrillation: kinetic mechanism and potential interpretation pitfalls. *J Am Chem Soc*. 2008; 130(1): 309-317. doi: 10.1021/ja076225s

43. Xu M, Ermolenkov VV, Uversky VN, Lednev IK. Hen egg white lysozyme fibrillation: A deep-UV resonance Raman spectroscopic study. *J Biophotonics*. 2008; 1(3): 215-229. doi: 10.1002/jbio.200710013

44. Xu M, Shashilov V, Lednev IK. Probing the cross-β core structure of amyloid fibrils by hydrogen−deuterium exchange deep ultraviolet resonance Raman spectroscopy. *Journal of the American Chemical Society*. 2007; 129(36): 11002-11003. doi: 10.1021/ja073798w

45. Manoharan R, Ghiamati E, Chadha S, Nelson W, Sperry J. Effect of cultural conditions on deep UV resonance Raman spectra of bacteria. *Applied Spectroscopy*. 1993; 47(12): 2145-2150. doi: 10.1366/0003702934066424

46. Chadha S, Manoharan R, Moënne-Loccoz P, Nelson W, Peticolas W, Sperry J. Comparison of the UV resonance Raman spectra of bacteria, bacterial cell walls, and ribosomes excited in the deep UV. *Applied Spectroscopy*. 1993; 47(1): 38-43. doi: 10.1366/0003702934048505

47. López-Díez EC, Goodacre R. Characterization of microorganisms using UV resonance Raman spectroscopy and chemometrics. *Analytical Chemistry*. 2004; 76(3): 585-591. doi: 10.1021/ac035110d

48. Lakowicz JR. *Principles of Fluorescence Spectroscopy* 3rd ed. New York City, USA: Springer Science; 2011.

49. Yang S, Li B, Slipchenko MN, et al. Laser wavelength dependence of background fluorescence in Raman spectroscopic analysis of synovial fluid from symptomatic joints. *J Raman Spectrosc*. 2013; 44(8): 1089-1095. doi: 10.1002/jrs.4338

50. Min Y-K, Yamamoto T, Kohda E, Ito T, Hamaguchi H-o. 1064 nm near-infrared multichannel Raman spectroscopy of fresh human lung tissues. *Journal of Raman Spectroscopy*. 2005; 36(1): 73-76. doi: 10.1002/jrs.1280

51. Amigo JM, Babamoradi H, Elcoroaristizabal S. Hyperspectral image analysis. A tutorial. *Anal Chim Acta*. 2015; 896: 34-51. doi: 10.1016/j.aca.2015.09.030

52. Cailleau R, Olivé M, Cruciger QV. Long-term human breast carcinoma cell lines of metastatic origin: Preliminary characterization. *In Vitro*. 1978; 14(11): 911-915. doi: 10.1007/BF02616120

53. Brinkley B, Beall P, Wible L, Mace M, Turner DS, Cailleau R. Variations in cell form and cytoskeleton in human breast carcinoma cells in vitro. *Cancer Res*. 1980; 40(9): 3118-3129.

54. Winnard Jr PT, Zhang C, Vesuna F, et al. Organ-specific isogenic metastatic breast cancer cell lines exhibit distinct Raman spectral signatures and metabolomes. *Oncotarget*. 2017; 8(12): 20266-20287. doi: 10.18632/oncotarget.14865

55. Joo KM, Park IH, Shin JY, et al. Human neural stem cells can target and deliver therapeutic genes to breast cancer brain metastases. *Mol Ther*. 2009; 17(3): 570-575. doi: 10.1038/mt.2008.290

56. Lednev IK, Ermolenkov VV, He W, Xu M. Deep-UV Raman spectrometer tunable between 193 and 205 nm for structural characterization of proteins. *Anal Bioanal Chem*. 2005; 381(2): 431-437. doi: 10.1007/s00216-004-2991-5

57. Talari ACS, Movasaghi Z, Rehman S, Rehman IU. Raman spectroscopy of biological tissues. *Applied Spectroscopy Reviews*. 2015; 50(1): 46-111. doi: 10.1080/05704928.2014.923902

58. Stone N, Kendall C, Shepherd N, Crow P, Barr H. Near-infrared Raman spectroscopy for the classification of epithelial pre-cancers and cancers. *Journal of Raman Spectroscopy*. 2002; 33(7): 564-573. doi: 10.1002/jrs.882

59. Bonnier F, Byrne H. Understanding the molecular information contained in principal component analysis of vibrational spectra of biological systems. *Analyst*. 2012; 137(2): 322-332. doi: 10.1039/c1an15821j

60. Ruiz-Chica A, Medina M, Sánchez-Jiménez F, Ramírez F. Characterization by Raman spectroscopy of conformational changes on guanine–cytosine and adenine–thymine oligonucleotides induced by aminooxy analogues of spermidine. *Journal of Raman Spectroscopy*. 2004; 35(2): 93-100. doi: 10.1002/jrs.1107

61. Chan JW, Taylor DS, Zwerdling T, Lane SM, Ihara K, Huser T. Micro-Raman spectroscopy detects individual neoplastic and normal hematopoietic cells. *Biophys J*. 2006; 90(2): 648-656. doi: 10.1529/biophysj.105.066761

62. Bhattacharjee T, Kumar P, Maru G, Ingle A, Krishna CM. Swiss bare mice: A suitable model for transcutaneous *in vivo* Raman spectroscopic studies of breast cancer. *Lasers Med Sci.* 2014; 29(1): 325-333. doi: 10.1007/s10103-013-1347-9

63. Dukor RK. Vibrational Spectroscopy in the Detection of Cancer. In: *Handbook of Vibrational Spectroscopy*. Hoboken, New Jersey, USA: John Wiley & Sons, Ltd; 2006.

64. Gaudreau P-O, Stagg J, Soulières D, Saad F. The present and future of biomarkers in prostate cancer: Proteomics, genomics, and immunology Advancements. *Biomarkers Cancer.* 2016; 8: (Suppl 2): 15–33. doi: 10.4137/BIC.S31802

65. Filella X, Fernández-Galan E, Bonifacio RF, Foj L. Emerging biomarkers in the diagnosis of prostate cancer. *Pharmgenomics Pers Med.* 2018; 11: 83-94. doi: 10.2147/PGPM.S136026

66. Burns-Cox N, Avery NC, Gingell JC, Bailey AJ. Changes in collagen metabolism in prostate cancer: A host response that may alter progression. *J Urol.* 2001; 166(5): 1698-1701. doi: 10.1016/S0022-5347(05)65656-X

67. Hall CL, Dai J, van Golen KL, Keller ET, Long MW. Type I collagen receptor (α2β1) signaling promotes the growth of human prostate cancer cells within the bone. *Cancer Research.* 2006; 66(17): 8648-8654. doi: 10.1158/0008-5472

68. Hall CL, Dubyk CW, Riesenberger TA, Shein D, Keller ET, van Golen KL. Type I collagen receptor (α2β1) signaling promotes prostate cancer invasion through RhoC GTPase. *Neoplasia.* 2008; 10(8): 797-803. doi: 10.1593/neo.08380

69. Crow P, Stone N, Kendall CA, et al. The use of Raman spectroscopy to identify and grade prostatic adenocarcinoma in vitro. *Br J Cancer.* 2003; 89: 106-108. doi: 10.1038/sj.bjc.6601059

70. Crow P, Barrass B, Kendall C, et al. The use of Raman spectroscopy to differentiate between different prostatic adenocarcinoma cell lines. *Br J Cancer.* 2005; 92(12): 2166-2170. doi: 10.1038/sj.bjc.6602638

71. Prensner JR, Rubin MA, Wei JT, Chinnaiyan AM. Beyond PSA: The next generation of prostate cancer biomarkers. *Sci Transl Med.* 2012; 4(127): 127rv123. doi: 10.1126/scitranslmed.3003180

72. Shetty G, Kendall C, Shepherd N, Stone N, Barr H. Raman spectroscopy: Elucidation of biochemical changes in carcinogenesis of oesophagus. *Br J Cancer.* 2006; 94(10): 1460-1464. doi: 10.1038/sj.bjc.6603102

73. Stone N, Kendall C, Smith J, Crow P, Barr H. Raman spectroscopy for identification of epithelial cancers. *Faraday Discuss.* 2004; 126: 141-157. doi: 10.1038/sj.bjc.6603102

74. Holdhoff M, Yovino SG, Boadu O, Grossman SA. Blood-based biomarkers for malignant gliomas. *J Neurooncol.* 2013; 113(3): 345-352. doi: 10.1007/s11060-013-1144-0

75. Khalil AA. Biomarker discovery: A proteomic approach for brain cancer profiling. *Cancer Sci.* 2007; 98(2): 201-213. doi: 10.1111/j.1349-7006.2007.00374.x

76. Schwartz SA, Weil RJ, Johnson MD, Toms SA, Caprioli RM. Protein profiling in brain tumors using mass spectrometry: Feasibility of a new technique for the analysis of protein expression. *Clin Cancer Res.* 2004; 10(3): 981-987. doi: 10.1158/1078-0432.CCR-0927-3

77. Kendall C, Day J, Hutchings J, et al. Evaluation of Raman probe for oesophageal cancer diagnostics. *Analyst.* 2010; 135(12): 3038-3041. doi: 10.1039/c0an00536c

78. Liu Z, Davis C, Cai W, He L, Chen X, Dai H. Circulation and long-term fate of functionalized, biocompatible single-walled carbon nanotubes in mice probed by Raman spectroscopy. *Proceedings of the National Academy of Sciences.* 2008; 105(5): 1410-1415. doi: 10.1073/pnas.0707654105

79. Huang Z, McWilliams A, Lui H, McLean DI, Lam S, Zeng H. Near-infrared Raman spectroscopy for optical diagnosis of lung cancer. *Int J Cancer.* 2003; 107(6): 1047-1052. doi: 10.1002/ijc.11500

80. Liu T, Chen C, Shi X, Liu C. Evaluation of Raman spectra of human brain tumor tissue using the learning vector quantization neural network. *Laser Physics.* 2016; 26(5): 055606.

81. Kalkanis SN, Kast RE, Rosenblum ML, et al. Raman spectroscopy to distinguish grey matter, necrosis, and glioblastoma multiforme in frozen tissue sections. *J Neurooncol.* 2014; 116(3): 477-485. doi: 10.1007/s11060-013-1326-9

82. Dabholkar MD, Berger MS, Vionnet JA, et al. Malignant and nonmalignant brain tissues differ in their messenger RNA expression patterns for ERCC1 and ERCC2. *Cancer Res.* 1995; 55(6): 1261-1266.

83. Shen L, Chen L, Wang Y, Jiang X, Xia H, Zhuang Z. Long noncoding RNA MALAT1 promotes brain metastasis by inducing epithelial-mesenchymal transition in lung cancer. *J Neurooncol.* 2015; 121(1): 101-108. doi: 10.1007/s11060-014-1613-0

84. Mahadevan-Jansen A, Richards-Kortum R. *Raman spectroscopy for cancer detection: A review.* Paper Presented at: Proceedings of the 19th Annual International Conference of the IEEE Engineering in Medicine and Biology Society. 30 Oct.-2 Nov, 1997; Chicago, IL, USA: doi: 10.1109/IEMBS.1997.756895

85. Bocklitz TW, Guo S, Ryabchykov O, Vogler N, Popp Jr. Raman based molecular imaging and analytics: A magic bullet for biomedical applications? *Anal Chem.* 2016; 88(1): 133-151. doi:

10.1021/acs.analchem.5b04665

86. Lednev IK. Biological Applications of Ultraviolet Raman Spectroscopy. In: Uversky VN, Permyakov EA, eds. *Methods in Protein Structure and Stability Analysis: Vibrational Spectroscopy*. Hauppauge, NY, USA: Nova Science Publishers, Inc.; 2007: 1-26.

87. Beaven G, Holiday E. Ultraviolet absorption spectra of proteins and amino acids. *Advances in Protein Chemistry*. 1952; 7: 319-386. doi: 10.1016/S0065-3233(08)60022-4

88. Wen ZQ, Thomas Jr GJ. UV resonance Raman spectroscopy of DNA and protein constituents of viruses: Assignments and cross sections for excitations at 257, 244, 238, and 229 nm. *Biopolymers*. 1998; 45(3): 247-256. doi: 10.1002/(SICI)1097-0282(199803)45:3<247::AID-BIP7>3.0.CO;2-R

89. Fodor SP, Copeland RA, Grygon CA, Spiro TG. Deep-ultraviolet Raman excitation profiles and vibronic scattering mechanisms of phenylalanine, tyrosine, and tryptophan. *Journal of the American Chemical Society*. 1989; 111(15): 5509-5518. doi: 10.1021/ja00197a001

90. Ziegler L, Hudson B, Strommen D, Peticolas W. Resonance Raman spectra of mononucleotides obtained with 266 and 213 nm ultraviolet radiation. *Biopolymers*. 1984; 23(10): 2067-2081. doi: 10.1002/bip.360231017

91. Fodor SP, Rava RP, Hays TR, Spiro TG. Ultraviolet resonance Raman spectroscopy of the nucleotides with 266-, 240-, 218-, and 200-nm pulsed laser excitation. *Journal of the American Chemical Society*. 1985; 107(6): 1520-1529. doi: 10.1021/ja00292a012

92. Voet D, Gratzer W, Cox R, Doty P. Absorption spectra of nucleotides, polynucleotides, and nucleic acids in the far ultraviolet. *Biopolymers*. 1963; 1(3): 193-208. doi: 10.1002/bip.360010302

93. International Commission on Non-Ionizing Radiation Protection. Guidelines on limits of exposure to ultraviolet radiation of wavelengths between 180 nm and 400 nm (incoherent optical radiation). *Health Phys*. 2004; 87(2): 171-186. doi: 10.1097/00004032-200408000-00006

94. Monici M. Cell and tissue autofluorescence research and diagnostic applications. *Biotechnol Annu Rev*. 2005; 11: 227-256. doi: 10.1016/S1387-2656(05)11007-2

95. Jamme F, Kascakova S, Villette S, et al. Deep UV autofluorescence microscopy for cell biology and tissue histology. *Biol Cell*. 2013; 105(7): 277-288. doi: 10.1111/boc.201200075

96. Cheng W-T, Liu M-T, Liu H-N, Lin S-Y. Micro-Raman spectroscopy used to identify and grade human skin pilomatrixoma. *Microsc Res Tech*. 2005; 68(2): 75-79. doi: 10.1002/jemt.20229

97. Kirschenbaum DM. Molar absorptivity and A 1% 1cm values for proteins at selected wavelengths of the ultraviolet and visible regions. XIII. *Anal Biochem*. 1977; 81(1): 220-246.

98. Angioni E, Lercker G, Frega NG, et al. UV spectral properties of lipids as a tool for their identification. *European Journal of Lipid Science and Technology*. 2002; 104(1): 59-64. doi: 10.1002/1438-9312(200201)104:1<59::AID-EJLT59>3.0.CO;2-I

99. Bykov VJ, Hemminki K. Assay of different photoproducts after UVA, B and C irradiation of DNA and human skin explants. *Carcinogenesis*. 1996; 17(9): 1949-1955.

100. Reisz JA, Bansal N, Qian J, Zhao W, Furdui CM. Effects of ionizing radiation on biological molecules—mechanisms of damage and emerging methods of detection. *Antioxid Redox Signal*. 2014; 21(2): 260-292. doi: 10.1089/ars.2013.5489

101. Gršković B, Zrnec D, Popović M, Petek MJ, Primorac D, Mršić G. Effect of ultraviolet C radiation on biological samples. *Croat Med J*. 2013; 54(3): 263-271. doi: 10.3325/cmj.2013.54.263